PRAMANA — journal of physics

Vol. 79, No. 2
August 2012
pp. 249–262

Measurement of ^{232}Th(n, γ) and ^{232}Th(n, $2n$) cross-sections at neutron energies of 13.5, 15.5 and 17.28 MeV using neutron activation techniques

SADHANA MUKERJI[1,*], H NAIK[2], S V SURYANARAYANA[3], S CHACHARA[1], B S SHIVASHANKAR[4], V MULIK[5], RITA CRASTA[6], SUDIPTA SAMANTA[1], B K NAYAK[3], A SAXENA[3], S C SHARMA[3], P V BHAGWAT[3], K K RASHEED[1], R N JINDAL[1], S GANESAN[1], A K MOHANTY[3], A GOSWAMI[2] and P D KRISHNANI[1]

[1]Reactor Physics Design Division; [2]Radiochemistry Division; [3]Nuclear Physics Division, Bhabha Atomic Research Centre, Mumbai 400 085, India

[4]Department of Statistics, Manipal University, Manipal 576 104, India

[5]Department of Physics, University of Pune, Pune 411 007, India

[6]Department of Studies in Physics, Microtron Centre, Mangalore University, Mangalagangotri 574 199, India

*Corresponding author. E-mail: mukerjis@barc.gov.in

MS received 22 November 2011; revised 29 January 2012; accepted 8 February 2012

Abstract. The ^{232}Th(n, γ) reaction cross-section at average neutron energies of 13.5, 15.5 and 17.28 MeV from the ^{7}Li(p, n) reaction has been determined for the first time using activation and off-line γ-ray spectrometric technique. The ^{232}Th(n, $2n$) cross-section at 17.28 MeV neutron energy has also been determined using the same technique. The experimentally determined ^{232}Th(n, γ) and ^{232}Th(n, $2n$) reaction cross-sections from the present work were compared with the evaluated data of ENDF/BVII and JENDL-4.0 and were found to be in good agreement. The present data, along with literature data in a wide range of neutron energies, were interpreted in terms of competition between ^{232}Th(n, γ), (n, f), (n, nf) and (n, xn) reaction channels. The ^{232}Th(n, γ) and ^{232}Th(n, $2n$) reaction cross-sections were also calculated theoretically using the TALYS 1.2 computer code and were found to be in good agreement with the experimental data from the present work but were slightly higher than the literature data at lower neutron energies.

Keywords. ^{232}Th(n, γ) and ^{232}Th(n, $2n$) reaction cross-sections; off-line γ-ray spectrometric technique; $E_{\mathrm{n}} = 13.5$, 15.5 and 17.28 MeV; ^{7}Li(p, n) reaction.

PACS No. 25.85

DOI: 10.1007/s12043-012-0299-0; ***e*Publication: 23 June 2012**

1. Introduction

Presently, advanced heavy water reactors (AHWR) [1,2] and fast reactors [3–6] are of interest for power production. Recently, accelerator-driven sub-critical systems (ADS) [7–12] are also of primary interest from the point of transmutation of long-lived fission products (^{93}Zr, ^{99}Tc, ^{107}Pd, ^{129}I and ^{135}Cs), and incineration of long-lived minor actinides (^{237}Np, ^{240}Pu, ^{241}Am, ^{243}Am and ^{244}Cm) to solve the problem of radioactive wastes. In AHWR, ^{232}Th–^{233}U is the primary fuel for power generation. However, ^{232}Th–^{233}U fuel in combination with ADS is another method for power generation besides for transmutation of long-lived fission products and incineration of long-lived minor actinides. The advantage of ^{232}Th–^{233}U fuel in AHWR [1,2] and ADS [7–12] over the present reactors based on uranium fuel is that it produces thousand times less radiotoxic wastes. Studies have shown that thorium-based fuels in fast spectrum systems can efficiently perform the task of reducing reactor-grade and weapons-grade plutonium stockpile [13] while maintaining acceptable safety and control characteristics of the reactor system. Besides these, thorium in the Earth's crust is three to four times more abundant than uranium and thus can help to greatly extend the nuclear fuel resources. It is a fact that ^{232}Th is the only nucleus present in nature which can give rise to an excess of fissile material ^{233}U in the presence of either thermal or fast neutrons, thus making it an excellent choice for nuclear reactors of the future. Furthermore, thorium-based fuel is an attractive option because no trans-uranics are produced compared to uranium-based fuels. This reduces the cost of fuel cycle.

In the thorium–uranium fuel cycle, the fissile nucleus ^{233}U is generated by ^{232}Th(n,γ)–^{233}Th reaction followed by two successive β-decays. The ^{232}Th$(n,2n)^{231}$Th reaction cross-section rapidly increases above a threshold energy of 6.648 MeV. A schematic diagram of the Th–U fuel cycle is given below:

$$
\begin{array}{ccccccc}
^{232}\mathrm{Th}\,(n,\gamma) & \rightarrow & ^{233}\mathrm{Th} & \xrightarrow{\beta^-} & ^{233}\mathrm{Pa} & \xrightarrow{\beta^-} & ^{233}\mathrm{U} \\
1.405\times10^{10}\ \mathrm{y} & & 22.3\ \mathrm{m} & & 26.97\ \mathrm{d} & & 1.52\times10^{5}\ \mathrm{y} \\
\downarrow_{(n,2n)} & & & & & & \downarrow_{(n,2n)} \\
^{231}\mathrm{Th} & \xrightarrow{\beta^-} & ^{231}\mathrm{Pa}\,(n,\gamma) & \rightarrow & ^{232}\mathrm{Pa} & \xrightarrow{\beta^-} & ^{232}\mathrm{U} \\
25.32\ \mathrm{h} & & 52760\ \mathrm{y} & & 1.31\ \mathrm{d} & & 68.7\ \mathrm{y}
\end{array}
$$

Thus, the production of the fissile nucleus ^{233}U depends on the ^{232}Th(n,γ) reaction cross-section, which is required with an accuracy of 1–2% for predicting the dynamical behaviour of complex arrangements in fast reactors or ADS [14,15]. In fusion–fission hybrid systems, a sensitivity study has shown that the production rate of ^{233}U can be predicted within 1%, provided the ^{232}Th(n,γ) cross-section is known within 2% [16,17]. Thus, the neutron interactions and fission cross-sections for ^{232}Th and ^{233}U in the low neutron energy are important for AHWR [1,2], whereas the neutron interactions and fission cross-sections in the higher energy range are important for ADS [7–12] because they dominate the neutron transport and neutron regeneration. Thus, the ^{232}Th(n,γ) reaction cross-section at higher neutron energy has a strong impact on the performance and safety assessment for ADS [18]. In ADS a 10% change in the ^{232}Th neutron capture cross-section gives rise to a 30% change in the needed proton current of the accelerator if the

system has to be operated at a sub-critical level of $K_{\text{eff}} \approx 0.97$ [19]. Thus, precise nuclear reaction cross-section data are important for the nuclear and shielding design of AHWR and ADS-based transmutation system. However, the database and experience of thorium fuels and the thorium fuel cycles are very limited compared to other conventional fuels.

A careful look at the nuclear cross-section data, available in the existing cross-section libraries shows that, $^{232}\text{Th}(n, \gamma)$ reaction cross-section data within neutron energies of thermal to 2.73 MeV are based on physical measurements [20–22] and activation technique [23–35]. Beyond 2.73 MeV, the $^{232}\text{Th}(n, \gamma)$ reaction cross-section data are available only at 3.7 and 9.85 MeV (Naik *et al* [36]) and at 14.5 MeV (Perkin *et al* [37]) using the activation technique. From these data, it can be seen that the $^{232}\text{Th}(n, \gamma)$ reaction cross-section decreases monotonically from 20 eV to 3.7 MeV. Beyond the neutron energy in the range of 6–7 MeV, $^{232}\text{Th}(n, \gamma)$ reaction cross-section increases and remains flat within 9.85–14.5 MeV [36,37]. It can also be seen from refs [36,37] that the $^{232}\text{Th}(n, \gamma)$ reaction cross-section at 14.5 MeV is higher than the expected trend. At neutron energy higher than 6.44 MeV, $^{232}\text{Th}(n, 2n)$ reaction begins and becomes the predominant mode besides fission and inelastic reaction channels, which are already significant above 1 MeV. In contrast to $^{232}\text{Th}(n, \gamma)$ reaction cross-section data [20–37], sufficient data on $^{232}\text{Th}(n, 2n)$ reaction are available from physical measurements [38] and from off-line activation methods [39–46]. However, the literature data of $^{32}\text{Th}(n, 2n)$ reaction cross-section [38–46] are within 11 MeV neutron energy. It can be seen from these data that the $^{232}\text{Th}(n, 2n)$ reaction cross-section increases from 6.44 MeV up to the neutron energy of 9.86 MeV and then remains constant up to 11 MeV. Keeping these facts in mind, it is important to measure the $^{232}\text{Th}(n, \gamma)$ and (n, xn) reaction cross-sections besides the yields of fission products at higher neutron energy.

In the present work, we have determined the $^{232}\text{Th}(n, \gamma)$ reaction cross-section at average neutron energies of 13.5 ± 0.35, 15.5 ± 0.5 and 17.28 ± 0.35 MeV using the neutron beam from $^{7}\text{Li}(p, n)$ reaction and by activation followed by off-line γ-ray spectrometry. The $^{232}\text{Th}(n, 2n)$ reaction cross-section is also determined at an average neutron energy of 17.28 ± 0.35 MeV using the same technique. The neutron interaction cross-sections in the energy range 14–18 MeV are of fundamental importance for fission and accelerator-driven reactors because they dominate the neutron transport and neutron regeneration. The present data along with literature data at different neutron energies, are interpreted from the point of view of (n, f), (n, nf), $(n, 2nf)$ and (n, xn) reaction thresholds.

2. Description of the experiment

The experiment was carried out in 14UD BARC-TIFR Pelletron Facility at Mumbai, India [36]. The neutron beam was obtained from the $^{7}\text{Li}(p, n)$ reaction by using the proton beam main line which was placed 6 m above the analysing magnet of the Pelletron Facility so as to utilize the maximum proton current from the accelerator. The energy spread for proton at 6 m height was the maximum (50–90 keV). At this port, the terminal voltage was regulated by GVM mode using terminal potential stabilizer. Further, we used a collimator of 6 mm diameter before the target. The lithium foil was made up of natural lithium having a thickness of 3.7 mg/cm^2 and was sandwiched between two tantalum foils of different thicknesses. The thinner tantalum foil having a thickness of 4 mg/cm^2 faced

the proton beam, in which the degradation of the proton energy was only 30 keV. The thicker tantalum foil of 1.0 mm, located behind the lithium foil, was sufficient to stop the proton beam. Behind the Ta–Li–Ta stack, the natural thorium metal foil of 1 cm^2 length and 0.025 mm thickness was placed for irradiation. The Th foil was wrapped with 0.025 mm thick superpure aluminum foil and mounted at zero degree with respect to the beam direction at a distance of 2.1 cm from the location of the Ta–Li–Ta stack. The experimental arrangement is shown in figure 1. The isotopic abundance of ^{232}Th in natural thorium is 100%. Different sets were made for different irradiations at various neutron energies.

The samples were irradiated for 5–7 h depending on the proton beam energy. The proton beam energies were 16, 18 and 20 MeV and the proton current during the irradiation was within 300–400 nA. The maximum incident neutron energies on Th targets were 14.1, 16.1 and 18.1 MeV respectively. After irradiation, the samples were cooled for sufficient time (6–24 h). Then the irradiated target of Th along with Al wrapper were mounted on different Perspex plates and taken for γ-ray spectrometry. The γ-ray counting of fission/reaction products from the irradiated Th sample was done at BARC using pre-calibrated HPGe detector connected to a PC-based 16 K GAMMA FAST MCA with High Voltage Power Supply Card. The detector is a coaxial p-type HPGe detector from EURASIS, France, with a relative efficiency of 50%. The resolution of the detector system was 2 keV at 1332.5 keV of ^{60}Co. The detector has a 3″ lead shielding on all sides to reduce the background of the system. The measurements were repeated several times to follow the decay of the radionuclides. Measurements were done at suitable distance between the sample and the end cap of the detector to keep the dead time within 5% to avoid pile-up effects. The γ-ray counting of the sample was done in live time mode and was followed as a function of time. The energy and efficiency calibration of the detector system was done by counting the γ-ray energies of standard ^{152}Eu and ^{133}Ba sources keeping the same geometry, where the summation error was negligible. The uncertainty in the efficiency was 2–3%. The γ-ray counting of the irradiated Th samples were done up to few months to check the half-life of the nuclides of interest. A typical γ-ray spectrum from the irradiated ^{232}Th sample for ^{232}Th(n, γ) and ^{232}Th$(n, 2n)$ reactions are given in figures 2 and 3 respectively.

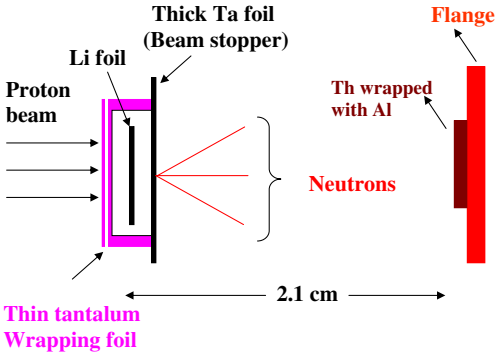

Figure 1. Schematic diagram showing the arrangement used for neutron irradiation.

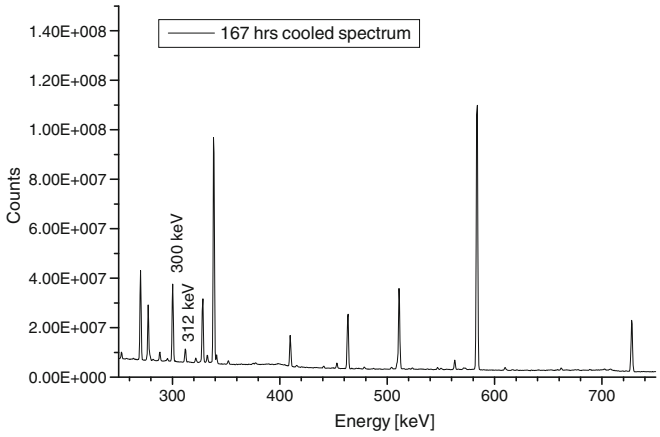

Figure 2. Typical γ-ray spectrum of irradiated natural Th metal showing the γ-ray spectrum for ^{232}Th(n,γ) reaction.

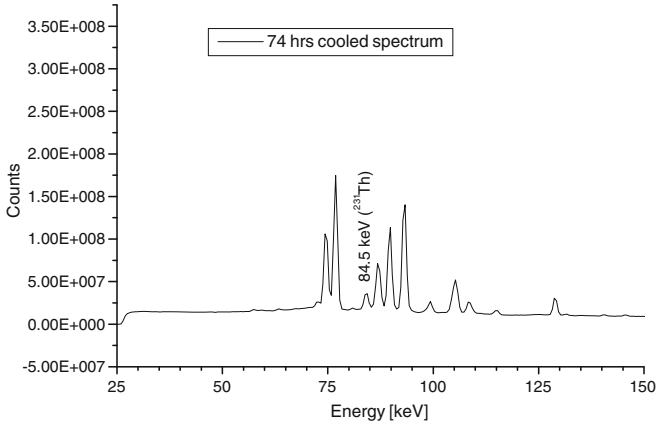

Figure 3. Typical γ-ray spectrum of irradiated natural Th metal showing γ-ray spectrum for ^{232}Th$(n,2n)$ reaction.

3. Analysis of the experiment

3.1 *Calculation of the neutron energy*

The incident proton energies in the present experiment were 16, 18 and 20 MeV respectively. The maximum incident neutron energies on Th targets were 14.1, 16.1 and 18.1 MeV respectively. Neutrons are generated by the ^{7}Li(p,n) reaction. However, a different reaction takes place when the proton beam heats the natural lithium target. Natural lithium consists of ^{6}Li and ^{7}Li isotopes with 7.42% and 92.58% abundances respectively. The Q-value for the ^{7}Li$(p,n)^7$Be reaction to the ground state is -1.644 MeV, whereas for the first excited state it is 0.431 MeV above the ground state leading to an average

Q-value of -2.075 MeV. The proton energies selected for the experiment are 16, 18 and 20 MeV. The degradation of the proton energy on the front thin tantalum foil of 4 mg/cm^2 thickness is only 30 keV. The ground state of ^{7}Be is having the threshold of 1.881 MeV, whereas the first excited state of ^{7}Be is having the threshold of 2.38 MeV. With ^{7}Li, a second neutron group at $E_P \geq 2.4$ MeV is produced due to the population of the first excited state of ^{7}Be. Thus, for proton energies of 16, 18 and 20 MeV, the corresponding first group of (n_0) neutron energies are 14.12, 16.12 and 18.12 MeV to the ground state of ^{7}Be. For the first excited state of ^{7}Be, the neutron energy of the second group of neutrons (n_1) will be 13.62, 15.62 and 17.62 MeV respectively. Fragmentation of $^7\mathrm{Li}(p,\gamma)^8\mathrm{Be}^* \rightarrow {}^4\mathrm{He} + {}^3\mathrm{He} + n$ ($Q = -3.23$ MeV) also occurs when the proton energy exceeds the value 4.5 MeV and the other reaction channels are open to give continuous neutron distribution besides n_0 and n_1 groups of neutrons. The branching ratio to the ground and first excited states of ^{7}Be up to the proton energy of 7 MeV is given in refs [47,48], whereas for proton energies from 4.2 MeV to 26 MeV is given in ref. [49]. For proton energies of 16, 18 and 20 MeV, the neutron spectra are continuous besides n_0 and n_1 group of neutrons. To observe the trend of continuous neutron spectrum, we have generated it by using the neutron energy distribution given in refs [49,50]. This distribution is obtained by shifting the peak by -0.5 MeV. So the peak of the distribution is around 18 MeV for proton energy of 20 MeV. This scaling has been done due to the fact that the maximum neutron energy from $^7\mathrm{Li}(p,n)$ reaction cannot exceed $E_P - 1.88$ MeV. Similarly, for $E_P = 16$ and 18 MeV runs, the corresponding neutron distributions are obtained by interpolation of the neutron distributions of Mashnik *et al* [50]. These neutron distributions have a quasimonoenergetic peak near $E_P - 1.88$ MeV and a long tailing towards lower energies, as shown for the typical case in figure 4 for proton energy of 20 MeV. After removing the tailing distribution, the average neutron energies under the quasimonoenergetic main peak region were obtained as 13.35 ± 0.35, 15.5 ± 0.5 and 17.28 ± 0.35 MeV for proton energies of 16, 18 and 20 MeV respectively. These average energies

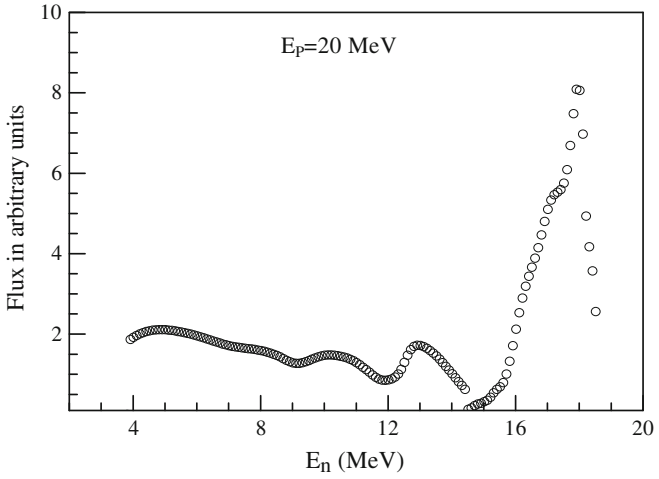

Figure 4. Plot of neutron flux in arbitrary unit as a function of neutron energy from $^7\mathrm{Li}(p,n)$ reaction for 20 MeV proton energy.

are the energy folded by flux under the main peak regions divided by the total flux under the peak.

3.2 *Calculation of the neutron flux*

For higher monoenergetic neutrons, the photopeak activity of the 336.2 keV γ-line of ^{115m}In from the ^{115}In(n, n') reaction is used for flux determination. In the present work, the neutron beam was produced from ^{7}Li(p, n) reaction, where the neutron energy is on the higher side and not exactly monoenergetic. This is due to the contribution from the second group as well as a tailing part from the break up $^{8}\text{Be} \rightarrow {}^{4}\text{He} + {}^{3}\text{He} + n$, which has a significant contribution. It can be seen from refs [49,50] that tailing region of the low-energy neutrons is quite significant. Within this range of neutron energy, the ^{115}In$(n, n')^{115m}$In reaction cross-sections change continuously [51]. On the other hand, the neutron-induced fission cross-section of ^{232}Th [52] has a step function, whereas the yields of fission products [53,54] at peak position of the mass-yield curve do not change significantly. For this purpose, the neutron flux [36] was calculated using the yield (Y) of fission products as ^{131}I, ^{132}Te and ^{97}Zr, extracted from the experimental yields of refs [53,54] in the neutron-induced fission of ^{232}Th. The neutron flux and the observed photopeak activities (A_{obs}) for γ-lines of the respective nuclide are related by the equation

$$\phi = \frac{A_{\text{obs}}\,(CL/LT)\,\lambda}{N\sigma_{\text{f}} Ya\varepsilon(1 - \text{e}^{-\lambda t})(\text{e}^{-\lambda T})(1 - \text{e}^{-\lambda CL})}, \tag{1}$$

where N is the number of target atoms σ_{f} is the fission cross-section taken from refs [55,56], Y is the yield of the fission product taken from refs [53,54], a is the branching intensity and ε is the detection efficiency for γ-lines of the nuclide of interest, t and T are the irradiation and cooling times whereas, CL is the clock time and LT is the live time of counting, respectively. In the above equation the CL/LT term has been used for dead time correction. The γ-ray energies and the nuclear spectroscopic data such as the half-lives and branching ratios of the reaction products are taken from refs [57–59] and given in table 1.

The neutron flux calculated using eq. (1) for 13.5 ± 0.35, 15.5 ± 0.5 and 17.28 ± 0.35 MeV neutron energies were $(9.65 \pm 0.76) \times 10^6$, $(3.09 \pm 0.25) \times 10^7$ and $(8.59 \pm 0.67) \times 10^7$ n cm^{-2} s^{-1} corresponding to the proton energies of 16, 18 and 20 MeV, respectively. The neutron flux for the ^{232}Th$(n, 2n)$ reaction at an average neutron energy of 17.28 ± 0.35 MeV was $(7.02 \pm 0.55) \times 10^7$ n cm^{-2} s^{-1}. This value was obtained

Table 1. Nuclear spectroscopic data used in the calculation.

Nuclide	Half-life	γ-ray energy (keV)	γ-ray abundance (%)	References
^{231}Th	25.52 h	84.2	6.6	[58,59]
^{233}Th	21.83 m	86.5	2.7	[58,59]
^{233}Pa	26.975 d	311.9	38.4	[58,59]

based on the ratio of the neutron flux of the neutron spectrum of refs [49,50] for $(n, 2n)$ reaction above its threshold to the total flux. The error for the neutron flux value is based on the propagated error from fission cross-section [52], yields of fission products [53,54] and the counting statistics of photopeak activity of the fission rate monitor.

3.3 *Determination of* $^{232}Th(n, \gamma)^{233}Th$ *and* $^{232}Th(n, 2n)^{231}Th$ *reaction cross-sections and their results*

The radioactive products such as ^{233}Th and ^{233}Pa were produced from ^{232}Th(n, γ) reaction followed by beta decay. Similarly, the radioactive product ^{231}Th was produced from the ^{232}Th$(n, 2n)$ reaction. For the calculation of ^{232}Th(n, γ) and ^{232}Th$(n, 2n)$ reaction cross-sections, the decay data of ^{233}Th, ^{233}Pa and ^{231}Th are taken from refs [57–59] and are shown in table 1. The radionuclide ^{233}Th ($t_{1/2} = 21.83$ m), which was produced by the ^{232}Th$(n, \gamma)^{233}$Th reaction underwent β^- decays to ^{233}Pa ($t_{1/2} = 26.975$ d). In view of this, the ^{232}Th(n, γ) reaction cross-section was calculated from the observed photopeak activity of ^{233}Pa in the γ-ray spectrum of the 7–15 days-cooled sample. So the ^{233}Pa radionuclide was identified through an analysis of the 311.9 keV characteristic γ-line. Similarly, the ^{232}Th$(n, 2n)$ reaction cross-section was calculated from the observed photopeak activity of the 84.2 keV γ-line of ^{231}Th in the γ-ray spectrum of a 12–25 h-cooled sample.

The number of detected γ-rays (A_{obs}) of the reaction products ^{233}Th and ^{231}Th was used to calculate the neutron-induced reaction cross-section of ^{232}Th using eq. (1) and is rewritten as

$$\sigma = \frac{A_{\text{obs}}\,(CL/LT)\,\lambda}{N\phi a\varepsilon(1 - \mathrm{e}^{-\lambda t})(\mathrm{e}^{-\lambda T})(1 - \mathrm{e}^{-\lambda CL})}. \tag{2}$$

All terms in eq. (2) have the same meaning as in eq. (1). In eq. (2) the experimentally obtained neutron flux mentioned before was used to calculate the ^{232}Th(n, γ) and ^{232}Th$(n, 2n)$ reaction cross-sections at different neutron energy. The ^{232}Th(n, γ) reaction cross-section for the average neutron energies of 13.5 ± 0.35, 15.5 ± 0.5 and 17.28 ± 0.35 MeV were 2.49 ± 0.15, 2.34 ± 0.15 and 1.569 ± 0.141 mb respectively. On the other hand, the ^{232}Th$(n, 2n)$ reaction cross-section at neutron energy of 17.28 ± 0.35 MeV was 656 ± 99 mb. The ^{232}Th(n, γ) cross-section values were slightly higher because of the contribution from the low-energy neutron reaction cross-section. The contribution of the cross-section due to the tail region of the neutron spectrum for the ^{232}Th(n, γ) reaction has been estimated using the ENDF/B-VII [60] and JENDL-4.0 [61] by folding the cross-sections with neutron flux distributions of refs [49,50]. At proton energies of 16, 18 and 20 MeV, the contribution of the cross-sections to the ^{232}Th(n, γ) reaction cross-section from ENDF/B-VII [60] was evaluated to be 1.402, 1.570 and 1.019 mb, respectively. On the other hand, the contribution of the cross-sections to the ^{232}Th(n, γ) reaction cross-section from JENDL-4.0 [61] for proton energies of 16, 18 and 20 MeV were 1.475, 1.709 and 1.113 mb, respectively. The actual experimentally obtained cross-sections for ^{232}Th(n, γ) reaction, after removing the contribution from the tail region, were 1.052 ± 0.166, 0.701 ± 0.171 and 0.501 ± 0.141 mb for average neutron energies of 13.5 ± 0.35, 15.5 ± 0.5 and 17.28 ± 0.35 MeV, which are given in table 2. At an

Table 2. ^{232}Th(n, γ) and $(n, 2n)$ reaction cross-sections at different neutron energies.

Neutron energy	Neutron flux	Cross-section (mb)		
(MeV)	(n cm^{-2} s^{-1})	Experimental	ENDF/B-VII	JENDL-4.0
			^{232}Th(n, γ)	
13.50 ± 0.35	$(9.65 \pm 0.76) \times 10^6$	1.052 ± 0.166	1.212–1.147[a]	1.398–1.136[a]
15.50 ± 0.5	$(3.09 \pm 0.25) \times 10^7$	0.701 ± 0.171	0.769–0.479[b]	0.962–0.773[b]
17.28 ± 0.35	$(8.59 \pm 0.67) \times 10^7$	0.503 ± 0.141	0.350–0.262[c]	0.692–0.556[c]
			^{232}Th$(n, 2n)$	
17.28 ± 0.35	$(7.02 \pm 0.55) \times 10^7$	656 ± 99	436–354[c]	676–533[c]

[a]For ^{232}Th(n, γ) reaction, the neutron energy ranges are 13–14 MeV.
[b]For ^{232}Th(n, γ) reaction, the neutron energy ranges are 15–16 MeV.
[c]For ^{232}Th(n, γ) and $(n, 2n)$ reaction, the neutron energy ranges are 17–18 MeV.

average neutron energy of 17.28 ± 0.35, corresponding to the proton energy of 20 MeV, the ^{232}Th$(n, 2n)^{231}$Th reaction cross-section was obtained to be 656 ± 99 mb, which is also given in table 2.

The uncertainties associated with the measured cross-sections come from the combination of two experimental data sets. This overall uncertainty is the quadratic sum of both statistical and systematic errors. The random error in the observed activity is primarily due to counting statistics, which is estimated to be 5–10%. This can be determined by accumulating the data for an optimum time period that depends on the half-life of the nuclides of interest. The systematic errors are due to uncertainties in photon flux estimation ($\sim$2%), the irradiation time ($\sim$0.5%), the detection efficiency calibration ($\sim$3%), the half-life of the reaction products and the γ-ray abundances ($\sim$2%) as reported in [57–59]. Thus, the total systematic error is about $\sim$4.2%. The overall uncertainty is found to range between 6.5 and 10.8%, coming from the combination of a statistical error of 5–10% and a systematic error of 4.2%.

4. Discussions

The ^{232}Th(n, γ) reaction cross-section at average neutron energies of 13.35 ± 0.35, 15.5 ± 0.5 and 17.28 ± 0.35 MeV (table 2) as well as the ^{232}Th$(n, 2n)$ reaction cross-section at an average neutron energy of 17.28 ± 0.35 MeV (table 2) from the present work are determined for the first time. The experimentally obtained reaction cross-sections for the ^{232}Th(n, γ) and ^{232}Th$(n, 2n)$ reactions are compared with the evaluated data from ENDF/B-VII [60] and JENDL-4.0 [61] and are given in table 2. These evaluated reaction cross-sections given in table 2 within the neutron energy range of 13–18 MeV for ^{232}Th(n, γ) reaction and 17–18 MeV for ^{232}Th$(n, 2n)$ reaction are due to the finite width of the neutron energy under the main peak [49,50].

The experimentally obtained ^{232}Th(n, γ) reaction cross-sections at average neutron energies of 13.5 ± 0.35, 15.5 ± 0.5 and 17.28 ± 0.35 MeV as well as the ^{232}Th$(n, 2n)$ reaction cross-section at a neutron energy of 17.28 ± 0.35 MeV are within the range of

the evaluated data (table 2). To examine this aspect, experimental data from [20–35] within the neutron energies of 1 keV to 2.7 MeV are plotted in figure 5. The experimental data at neutron energies of 3.7 and 9.85 MeV from ref. [36] as well as at 14.5 MeV from ref. [37] are also shown in figure 5. In the same figure, the evaluated data from ENDF/B-VII [60] and JENDL-4.0 [61] are also plotted for comparison. It can be seen from figure 5 that there are no data in the energy range of the present work except the data at 14.5 MeV [37]. The experimental data at 14.5 MeV are based on the neutron energy from D+T reaction and are significantly higher than the value of present work within neutron energy of 13.5–15.5 MeV. It can be seen from figure 5 that both experimental and evaluated ^{232}Th(n, γ) reaction cross-sections decrease up to a neutron energy of 6–7 MeV and thereafter increase up to 8 MeV and remain flat within neutron energy of 9–14 MeV. Lower value of ^{232}Th(n, γ) reaction cross-section around neutron energy of 6–7 MeV is due to the opening of ^{232}Th$(n, 2n)$ reaction channel having a threshold of 6.44 MeV. However, higher value of the ^{232}Th(n, γ) reaction cross-section at neutron energy above 8 MeV and near constant value within 9–14 MeV may be due to the saturation of $(n, 2n)$ and (n, nf) reactions cross-sections. In view of this, the ^{232}Th(n, γ) and ^{232}Th$(n, 2n)$ reaction cross-sections at neutron energy beyond 1 keV were calculated using the computer code TALYS, version 1.2 [62].

TALYS is a computer code basically used for analysing basic scientific experiments or for generating nuclear reaction cross-section data based on physics model parametrizations. The basic objective is the simulation of nuclear reactions that involve projectiles like photons, neutrons, protons, deuterons, tritons, ^{3}He- and α-particles, in the energy range of 1 keV to 200 MeV and for target nuclides of mass heavier than 12 amu. In the present work, we have used neutron energies from 1 keV to 20 MeV for ^{232}Th target. In TALYS, the cross-section for reactions to all open channels is calculated. Several options are included for the choice of different parameters such as γ-strength functions, nuclear level densities, nuclear model parameters etc. All outgoing channels possible for the given

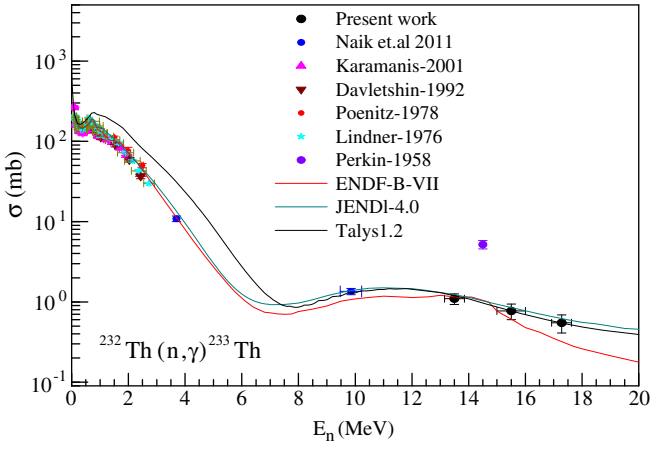

Figure 5. Plot of experimental, theoretical and evaluated ^{232}Th(n, γ) reaction cross-sections as a function of neutron energy.

neutron energy, including inelastic and fission channels, were considered. However, the cross-sections for the (n,γ) and $(n,2n)$ reactions were specially looked for and collected. Theoretically calculated ^{232}Th(n,γ) reaction cross-section using TALYS 1.2 computer code is also plotted in figure 5.

It can be seen from figure 5 that, the trend of the experimental and evaluated ^{232}Th(n,γ) reaction cross-sections is well reproduced by the TALYS 1.2 computer code. However, the ^{232}Th(n,γ) reaction cross-section calculated from TALYS are slightly higher than the experimental and evaluated data for neutron energies of 100 keV to 7.5 MeV but are comparable with the experimental values at neutron energies of 9.85 to 17.28 MeV. This is because in the TALYS the fission cross-section as a function of the neutron energy is quantitatively not well accounted, though the trend is reproduced. Similar to the evaluated data, the ^{232}Th(n,γ) reaction cross-section calculated using TALYS 1.2 code shows a dip in 6–7 MeV neutron energy. The dip in the ^{232}Th(n,γ) reaction cross-section around 6–7 MeV neutron energy indicates the opening of the $(n,2n)$ reaction channel besides the (n,nf) channel. To verify this, ^{232}Th$(n,2n)$ reaction cross-sections from the present work and from [38–46] along with the calculated [62] and evaluated data [60,61] are plotted in figure 6.

It can be seen from figure 5 that the experimental and calculated ^{232}Th$(n,2n)$ reaction cross-sections show a sharp increase from 6.6 MeV to 8.0 MeV neutron energy and thereafter remains constant up to 14 MeV. Thus, the increasing trend of ^{232}Th(n,γ) reaction cross-section beyond 8 MeV (figure 5) is due to the constant ^{232}Th$(n,2n)$ reaction cross-section (figure 6). Furthermore, it can be seen from figures 5 and 6 that the ^{232}Th(n,γ) reaction cross-section shows a dip, whereas the ^{232}Th$(n,2n)$ reaction cross-section shows a sharp increase. This is most probably due to the sharing of the excitation energy between ^{232}Th(n,γ) and $(n,2n)$ reaction channels in the neutron energy below 14 MeV. Above

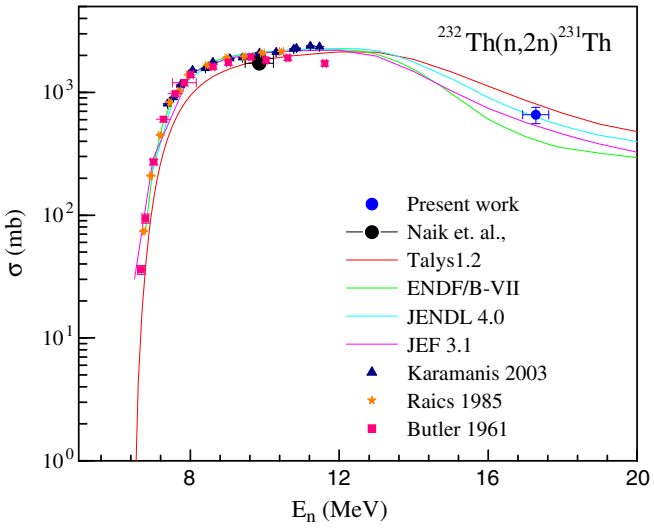

Figure 6. Plot of experimental, theoretical and evaluated ^{232}Th$(n,2n)$ reaction cross-sections as a function of neutron energy.

14 MeV neutron energy, ^{232}Th(n, γ) and $(n, 2n)$ reaction cross-sections show a decreasing trend due to the opening of $(n, 3n)$ reaction channels.

5. Conclusions

(i) The ^{232}Th$(n, \gamma)^{233}$Th reaction cross-sections at average neutron energies of 13.5 ± 0.35, 15.5 ± 0.5 and 17.28 ± 0.35 MeV as well as the ^{232}Th$(n, 2n)^{231}$Th reaction cross-section at 17.28 ± 0.35 MeV neutron energy have been determined for the first time.

(ii) The ^{232}Th(n, γ) and ^{232}Th$(n, 2n)$ reaction cross-sections at average neutron energies of 13.5 ± 0.35, 15.5 ± 0.5 and 17.28 ± 0.35 MeV are in good agreement with the evaluated data from ENDF/B-VII and JENDL-4.0.

(iii) The ^{232}Th(n, γ) and ^{232}Th$(n, 2n)$ reaction cross-sections were also calculated using the TALYS 1.2 computer code and found to be in general agreement with the experimentally determined values.

Acknowledgements

The authors would like to express their sincere thanks to the staff of the BARC-TIFR Pelletron Facility, for their cooperation during experiment. One of the authors (Sadhana Mukerji) is thankful to B Krishnamohan and Rajeev Sharma of Reactor Physics Design Division for their cooperation.

References

[1] R K Sinha and A Kakodkar, *Nucl. Eng. Des.* **236**, 7, 683 (2006)

[2] S Ganesan, Creation of Indian experimental benchmarks for thorium fuel cycle, IAEA coordinated research project on "Evaluated Data for Thorium-Uranium Fuel Cycle," Third Research Coordination Meeting, 30 January to 2 February 2006, Vienna, Austria, INDC (NDS)-0494 (2006)

[3] L Mathieu *et al*, Proportion for a very simple thorium molten salt reactor, *Proc. Global International Conference*, Paper No. 428 (Tsukuba, Japan, 2005)

[4] Fast reactors and accelerator driven systems knowledge base, IAEA-TECDOC-1319: Thorium fuel utilization: Options and trends

[5] A Nuttin, D Heuer, A Billebaud, R Brissot, C Le Brun, E Liatard, J M Loiseaux, L Mathieu, O Meplan, E Merle-Lucotte, H Nifenecker, F Perdu and S David, *Proc. Nucl. Energy* **46**, 77 (2005)

[6] T R Allen and D C Crawford, Science and Technology of Nuclear Installations, Article ID 97486 (2007)

[7] F Carminati, R Klapisch, J P Revol, Ch Roche, J A Rubio and C Rubbia, *An energy amplifier for cleaner and inexhaustible nuclear energy production driven by particle beam accelerator*, CERN Report No. CERN/AT/93-47 (ET) (1993)

[8] C Rubbia, J A Rubio, S Buono, F Carminati, N Fietier, J Galvez, C Geles, Y Kadi, R Klapisch, P Mandrilion, J P Revol, and Ch Roche, *Conceptual design of a fast neutron operated high power energy amplifier*, CERN/AT/95-44 (ET) (1995)

[9] American Institute of Physics Conference Proceedings, *The International Conference on Accelerator-Driven Transmutation Technologies and Applications* (Las Vegas, Nevada, USA, 1994) Vol. 346
[10] Accelerator Driven Systems: Energy Generation and Transmutation of nuclear waste, Status Report: IAEA- TECDOC- 985 (Nov. 1997)
[11] C D Bowman, *Ann. Rev. Nucl. Part. Sci.* **48**, 505 (1998)
[12] S Ganesan, *Pramana – J. Phys.* **68**, 257 (2007)
[13] K Yamashita, K Tokuhara and N Fujimoto, *Nucl. Sci. Eng.* **126**, 94 (1997)
[14] V G Pronyaev, Summary report of the consultants' meeting on assessment of nuclear data needs for thorium and other advanced cycles, INDC (NDS)-408, International Atomic Energy Agency (1999)
[15] B D Kuz'minov and V N Manokhin, *Nucl. Constants* **3–4**, 41 (1997)
[16] E T Cheng and D R Mathews, The influence of nuclear data uncertainties on thorium fusion-fission hybrid blanket nucleonic performance, *Proc. Int. Conf. Nuclear Cross Sections for Technology* (Knoxville, Tennessee, October 22–26, 1979) p. 834, NBS-SP 594, National Bureau of Standards
[17] D E Bartine, The use of thorium in fast breeder reactors, *Proc. Int. Conf. Nuclear Cross Sections for Technology* (Knoxville, Tennessee, October 22–26, 1979) p. 119, NBS-SP 594, National Bureau of Standards
[18] S Pelloni, G Youinou and P Wydler, Impact of different nuclear data on the performance of fast spectrum based on the thorium-uranium fuel cycle, *Proc. Int. Conf. Nuclear Data for Science and Technology* (Trieste, Italy, May 19–24, 1997) Part II, p. 1172
[19] M Salvatores, 'Experimental Facilities, Training and Expertise in the Nuclear Data Field: Needs and gaps for reactor physics applications,' Nuclear Data for Science and Technology (*Proc. Int. Conf. Trieste, 1997*), Vol. 59, Part I (G Reffo, A Ventura, and C Grandi (Eds.) (Italian Physical Society, Bologna, 1997) 3–17
[20] R C Little, R C Block, D R Harris, R E Slovacek and O N Carlson, *Nucl. Sci. Eng.* **79**, 175 (1981)
[21] A Borella, K Volev, A Brusegan, P Schillebeeckx, F Corvi, N Koyumdjieva, N Janeva and A A Lukyanov, *Nucl. Sci. Eng.* **152**, 1 (2006)
[22] G Aerts *et al*, *Phys. Rev.* **C73**, 054610 (2006)
[23] H Pomerance, *Phys. Rev.* **88**, 412 (1952)
[24] R L Macklin, N H Lazar and W S Lyon, *Phys. Rev.* **107**, 504 (1957)
[25] J A Miskel, K V Marsh, M Lindner and R J Nagle, *Phys. Rev.* **128**, 2717 (1962)
[26] D C Stupegia, B Smith and K Hamm, *J. Inorg. Nucl. Chem.* **25**, 627 (1963)
[27] M C Muxon, TRDWP/P-8, UK Atomic Energy Authority, Harwell (1963)
[28] L Forman, A D Schelberg, J H Warren and N W Glass, *Phys. Rev. Lett.* **27**, 117 (1971)
[29] V B Chelnokov *et al*, USSR Obninsk Report Jaderno Fizicheskii Issledovanija-13 P. 16 (Oct. 1972)
[30] M Lindner, R J Nagle and J H Landrum, *Nucl. Sci. Eng.* **59**, 381 (1976)
[31] R E Chrien, H I Liou, M J Kenny and M L Stelts, *Nucl. Sci. Eng.* **72**, 202 (1979)
[32] G T Baldwin and G F Knoll, *Nucl. Sci. Eng.* **88**, 123 (1984)
[33] R T Jones, J S Merritt and A Okazaki, *Nucl. Sci. Eng.* **93**, 171 (1986)
[34] K Wisshak, F Voss and F Kappeler, *Nucl. Sci. Eng.* **137**, 183 (2001)
[35] D Karamanis, M Petit, S Andriamonje, G Barreau, M Bercion, A Billebaud, B Blank, S Czajkowski, R Del Moral, J Giovinazzo, V Lacoste, C Marchand, L Perrot, M Pravikoff and J C Thomas, *Nucl. Sci. Eng.* **139**, 282 (2001)
[36] H Naik, P M Prajapati, S V Surayanarayana, K C Jagadeesan, S V Thakare, D Raj, V K Mulik, B S Sivashankar, B K Nayak, S C Sharma, S Mukherjee, Sarbjit Singh, A Goswami, S Ganesan and V K Manchanda, *Eur. Phys. J.* **A47**, 51 (2011)

[37] J L Perkin, L P O'connor and R F Colemann, *Proc. Phys. Soc. (London)* **72**, 505 (1958)
[38] R J Prestwood and B P Bayhurst, *Phys. Rev.* **121**, 1438 (1961)
[39] J P Butler and D C Santry, *Can J. Chem.* **39**, 689 (1961)
[40] R Batchelor, W B Gilboy and J H Towle, *Nucl. Phys.* **65**, 236 (1965)
[41] M Bormann, *Nucl. Phys.* **65**, 257 (1965)
[42] H Karius, A Ackermann and W Scobel, *J. Phys.* **G5**, 715 (1979)
[43] H Chatani, *Nucl. Instrum. Methods* **205**, 501 (1983)
[44] P Raics, S Daroczy, J Csikai, N V Kornilov, V Ya Baryba and O A Salnikov, *Phys. Rev.* **C32**, 87 (1985)
[45] The n-TOF Collaboration: D Karamanis, S Andriamonje, P A Assimakopoulos, G Dourkellis, D A Karademos, A Karydas, M Kokkoris, S Korrssionides, N G Nicolis, C Papachristodoulou, C T Papadopoulos, N Patronis, P Pavlopulous, G Perdikakis and R Vlastos, *Nucl. Instrum. Methods Phys. Res.* **A505**, 381 (2003)
[46] J Adam, A R Balabekyan, V S Barashenkov, R Brandt, V M Golovatiouk, V G Kalinnikov, K Katovosky, M I Krivopustov, V Kumar, H Kumawat, R Odoj, V S Pronskikh, A A Solnyshkin, V I Stegailov, V M Tsoupko-Sitnikov and W Westmeier, *Eur. Phys. J.* **A23**, 61 (2005)
[47] H Liskien and A Paulsen, *At. Data Nucl. Data Tables* **15**, 57 (1975)
[48] J W Meadows and D L Smith, *Neutrons from proton bombardment of natural lithium*, Argonne National Laboratory Report ANL-7983 (1972)
[49] C H Poppe, J D Anderson, J C Davis, S M Grimes and C Wong, *Phys. Rev.* **C14**, 438 (1976)
[50] S G Mashnik, M B Chadwick, H G Hughes, R C Little, R E Macfarlane, L S Waters and P G Young, ^{7}Li(*p*,*n*) *Nuclear data library for incident proton energies to 150 MeV*, Los Alamos National Laboratory, Los Alamos, NM 87545, USA (February 8, 2008)
[51] The international reactor dosimetry file:IRDF-2002 (Nuclear Data Section, International Atomic Energy Agency, 2002)
[52] J Blons, C Mazur and D Paya, *Phys. Rev. Lett.* **35**, 1749 (1975)
[53] L E Glendenin, J E Gindler, I Ahmad, D J Henderson and J W Meadows, *Phys. Rev.* **C22**, 152 (1980)
[54] E A C Crouch, *At. Data. Nucl. Data Tables* **19**, 419 (1977)
[55] R L Henkel, *Fast neutron cross sections: Corrections to LA-1714 and a correlation of 3 MeV values*, Los Alamos Scientific Lab. Reports No. LA-2122 (1957)
[56] C Paradels *et al*, *Advances in Nucl. Analysis and Simul*. (PHYSOR2006) (Vancouver, Canada, 2006) p. B076
[57] J Blachot, *Nucl. Data Sheets* **104**, 967 (2005)
[58] B Singh, J K Tuli, *Nucl. Data Sheets* **105**, 109 (2005)
[59] E Browne, *Nucl. Data Sheets* **93**, 763 (2001)
E Browne and R B Firestone, *Table of radioactive isotopes* edited by V S Shirley (John Wiley and Sons, New York, 1986)
[60] M B Chadwick *et al*, *Nucl. Data Sheets* **107**, 2931 (2006)
[61] K Shibata *et al*, *J. Nucl. Sci. Technol.* **48**, 1 (2011)
[62] A J Koning, S Hilaire and M C Duijvestijn, *Proceedings of the International Conference on Nuclear Data for Science and Technology*, ND 2004 (Santa Fe, 2004) edited by R C Haight, M B Chadwick, T Kawano and P Talou, *AIP Conf. Proc*. **769**, 1154 (2005)